

Branched covers and pencils on hyperelliptic Lefschetz fibrations

By Terry FULLER

(Received Nov. 99, 20XX)
(Revised Jan. 99, 20XX)

Abstract. For every fixed $h \geq 1$, we construct an infinite family of simply connected symplectic 4-manifolds $X'_{g,h}[i]$, for all $g > h$ and $0 \leq i < 2p - 1$, where $p = \lfloor \frac{g+1}{h+1} \rfloor$. Each manifold $X'_{g,h}[i]$ is the total space of a symplectic genus g Lefschetz pencil constructed by an explicit monodromy factorization. We then show that each $X'_{g,h}[i]$ is diffeomorphic to a complex surface that is a fiber sum formed from two standard examples of hyperelliptic genus h Lefschetz fibrations, here denoted Z_h and H_h . Consequently, we see that Z_h, H_h , and all fiber sums of them admit an infinite family of explicitly described Lefschetz pencils, which we observe are different from families formed by the degree doubling procedure.

1. Introduction

This paper is a sequel to [5] and [13]. In the former work, R. İnanç Baykur, Kenta Hayano, and Naoyuki Monden introduced a family of symplectic 4-manifolds $X'_g[i]$ for all $g \geq 3$ and $0 \leq i \leq g - 1$, each of which admits a genus g Lefschetz pencil with $2(i + 1)$ base points. In [5] they showed that this family has many interesting properties, among them potential exotic symplectic Calabi-Yau manifolds. (Here, “exotic” means not diffeomorphic to the standard K3 surface.) In [13], the author proved that in fact all of their examples are diffeomorphic to elliptic surfaces, and in particular that the symplectic Calabi-Yau manifolds in their list are standard. Although the Baykur-Hayano-Monden examples failed to yield new manifolds, the result in [13] revealed a rich collection of pencil structures on elliptic surfaces, described in an explicit way, as the manifolds $X'_g[i]$ were defined concretely through monodromy factorizations.

In the study of Lefschetz fibrations and pencils, hyperelliptic ones have been a particular object of focus, in part because they can be viewed as generalizations of genus 1 and 2 fibrations, where classification results exist. (See [19], [6], [22], [21].) It is known that every hyperelliptic Lefschetz fibration is a 2-fold branched cover of a rational surface ([12], [20]), allowing methods that will be at the core of the present article. Bernd Siebert and Gang Tian conjecture that every hyperelliptic Lefschetz fibration over S^2 without reducible fibers is holomorphic. They have settled this in fiber genus 2 for fibrations with transitive monodromy ([21]), and in this case it follows that every such fibration is equivalent to a fiber sum of two particular examples. The generalizations of these specific examples to arbitrary genus are studied in this paper.

These examples, to be denoted Z_h and H_h , arise from the well-known odd chain and hyperelliptic relations in the mapping class group $\text{Mod}(\Sigma_h)$ of a closed genus h surface. In Section 2 we define these manifolds, and review their topology; for H_h , we

also derive an equivalent monodromy factorization. Next, in Section 3, we generalize the mapping class group factorizations of Baykur, Hayano, and Monden from [5]. By performing unchaining surgeries on this factorization we construct for all fixed $h \geq 1$ a family $X'_{g,h}[i]$ of symplectic Lefschetz pencils, for all $g > h$ and $0 \leq i < 2p - 1$, where $p = \lfloor \frac{g+1}{h+1} \rfloor$. (The original Baykur-Hayano-Monden examples correspond to $h = 1$.) Our main theorem appears in Section 4, where we generalize the diffeomorphisms constructed in [13] to show that the total space of all of these pencils are diffeomorphic to complex surfaces obtained as fiber sums of the hyperelliptic examples Z_h and H_h . (The number of summands are determined by the divisor and remainder when $2g+2$ is divided by $2h+2$.) As was the case in [13], the proof relies on using Lefschetz fibration and pencil structures to depict the manifolds as 2-fold branched covers of rational surfaces; the diffeomorphism is described entirely in the base of these covers, using traditional Kirby calculus enhanced with moves that modify the branch set by isotopy. As a consequence, Z_h, H_h , and all fiber sums of them admit an infinite family of explicitly described Lefschetz pencils. In the final section, we make some remarks comparing these families to those produced by degree doubling, and speculate on possible applications to open questions in smooth and symplectic 4-manifold topology.

We assume the reader is familiar with the basic topology of Lefschetz fibrations and pencils on symplectic 4-manifolds. The preeminent reference for this topic is [15]. Careful summaries of background most relevant here also appear in the introductory sections of [5] and [13].

We denote a genus g surface with m marked points and n boundary components by $\Sigma_{g,m}^n$. A right-handed Dehn twist about a simple closed curve c on $\Sigma_{g,m}^n$ is denoted by t_c . The mapping class group of $\Sigma_{g,m}^n$ is denoted as $\text{Mod}(\Sigma_{g,m}^n)$. If m or n are omitted, they are assumed to be zero. Our convention is to multiply mapping classes left-to-right, that is $[\phi][\psi] = [\psi \circ \phi]$ for diffeomorphisms $\phi, \psi : \Sigma_{g,m}^n \rightarrow \Sigma_{g,m}^n$.

2. Two standard hyperelliptic Lefschetz fibrations

In this section, we survey the basic properties of two families of hyperelliptic Lefschetz fibrations. The curves c_i are indicated in Figure 1.

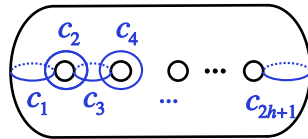


Figure 1. The curves c_1, \dots, c_{2h+1}

2.1. The manifolds Z_h

Let Z_h denote the total space of the genus h Lefschetz fibration over S^2 with monodromy given by the full odd chain relation $(t_{c_1} t_{c_2} \cdots t_{c_{2h+1}})^{2h+2} = 1$ in $\text{Mod}(\Sigma_h)$. These manifolds are simply connected, with Euler characteristic $e(Z_h) = 2(2h^2 + h + 3)$ and signature $\sigma(Z_h) = -2(h+1)^2$ ([9]). The odd chain relation lifts to the relation $(t_{c_1} t_{c_2} \cdots t_{c_{2h+1}})^{2h+2} = t_\delta t_{\delta'}$ in $\text{Mod}(\Sigma_h^2)$, where δ and δ' are curves parallel to the boundary components. Consequently, the fibration on Z_h admits two sections of square -1 ,

and blowing these down results in a pencil on a manifold denoted Z'_h . The manifolds Z_h and Z'_h are complex surfaces of general type for $h \geq 2$, and Z'_h is spin if and only if h is even.

Let C_n denote the ribbon surface in Figure 2. Using the methods of [12], we can

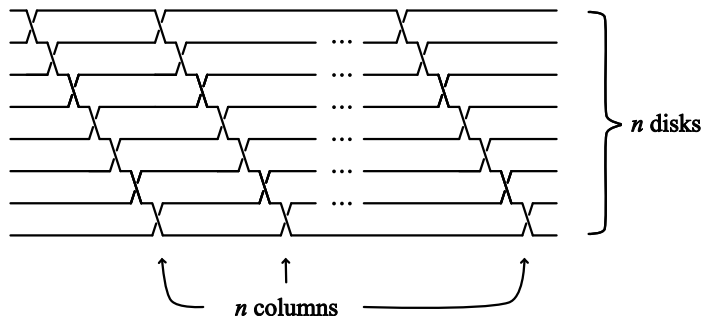


Figure 2. The ribbon surface C_n is obtained by attaching half-twisted bands to n parallel disks as shown.

describe Z_h as the 2-fold branched cover of $\mathbb{CP}^2 \# \overline{\mathbb{CP}^2}$ branched over the surface in Figure 3. Briefly summarized, in this figure the branch surface is a closed surface described

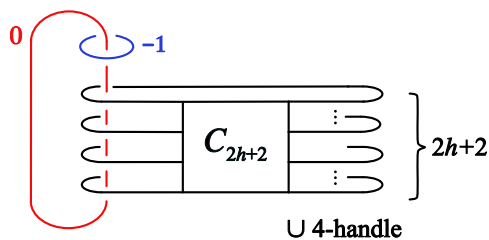


Figure 3. The 2-fold branched cover is Z_h .

as a banded unlink diagram, so that the full surface consists of the visible ribbon surface in Figure 3 union $2h + 2$ invisible disks in the 4-handle attached to the boundary of the ribbon surface. The framing of the -1 -framed 2-handle, as well as the fact that it does not intertwine with the ribbon branch surface, follows by considering the projection of the odd chain relation to the mapping class group $\text{Mod}(\Sigma_{0,2h+2})$ under the 2-fold branched cover $\Sigma_h \rightarrow \Sigma_{0,2h+2}$. Each Dehn twist t_{c_i} projects to a standard generator σ_i of $\text{Mod}(\Sigma_{0,2h+2})$ given by a right-handed disk twist about an arc that directly connects the i th and $(i + 1)$ st marked points. Let D_{2h+2}^2 be a disk in $\Sigma_{0,2h+2}$ that contains all of the marked branch points, and let $*$ be a point in the complement of D_{2h+2}^2 . The handle attachment can be understood by tracking a framed neighborhood of $*$ through an isotopy of the projection to the identity. (See [13] for a more complete explanation of this detail.) Here, the projection $(\sigma_1 \cdots \sigma_{2h+1})^{2h+2}$ is isotopic to a right-handed Dehn twist about a simple closed curve that encloses all of the marked branch points; this is isotopic to the identity on the sphere by an isotopy that fixes $*$ while rotating a neighborhood of $*$ once in a left-handed direction.

2.2. The manifolds H_h

Let H_h denote the genus h Lefschetz fibration with monodromy given by the hyperelliptic relation $(t_{c_1} t_{c_2} \cdots t_{c_{2h+1}} t_{c_{2h+1}} \cdots t_{c_2} t_{c_1})^2 = 1$ in $\text{Mod}(\Sigma_h)$. It is well-known that H_h is diffeomorphic to the rational surface $\mathbb{C}\mathbb{P}^2 \# (4h+5)\overline{\mathbb{C}\mathbb{P}^2}$, from which it easily follows that H_h is simply connected with Euler characteristic $e(H_h) = 4(h+2)$ and signature $\sigma(H_h) = -4(h+1)$.

We denote the (untwisted) fiber sum of r copies of H_h as $H_h(r)$, and use a similar notation for fiber sums of Z_h . We next describe an equivalent factorization for the Lefschetz fibrations in the family $H_h(r)$. The symbol \sim denotes Hurwitz equivalence of positive factorizations.

LEMMA 1. *For all $n \geq 1$, in $\text{Mod}(\Sigma_h)$ we have*

$$(t_{c_1} t_{c_2} \cdots t_{c_{2h+1}} t_{c_{2h+1}} \cdots t_{c_2} t_{c_1})^n \sim (t_{c_1} t_{c_2} \cdots t_{c_{2h+1}})^n (t_{c_{2h+1}} \cdots t_{c_2} t_{c_1})^n.$$

PROOF. Induction on n . The case where $n = 1$ is a tautology. Assuming the statement for $n - 1$, we then have

$$\begin{aligned} & (t_{c_1} t_{c_2} \cdots t_{c_{2h+1}} t_{c_{2h+1}} \cdots t_{c_2} t_{c_1})^n \\ &= (t_{c_1} t_{c_2} \cdots t_{c_{2h+1}} t_{c_{2h+1}} \cdots t_{c_2} t_{c_1})^{n-1} (t_{c_1} t_{c_2} \cdots t_{c_{2h+1}} t_{c_{2h+1}} \cdots t_{c_2} t_{c_1}) \\ &\sim (t_{c_1} t_{c_2} \cdots t_{c_{2h+1}}) (t_{c_1} t_{c_2} \cdots t_{c_{2h+1}} t_{c_{2h+1}} \cdots t_{c_2} t_{c_1})^{n-1} (t_{c_{2h+1}} \cdots t_{c_2} t_{c_1}) \\ &\sim (t_{c_1} t_{c_2} \cdots t_{c_{2h+1}}) (t_{c_1} t_{c_2} \cdots t_{c_{2h+1}})^{n-1} (t_{c_{2h+1}} \cdots t_{c_2} t_{c_1})^{n-1} (t_{c_{2h+1}} \cdots t_{c_2} t_{c_1}) \\ &= (t_{c_1} t_{c_2} \cdots t_{c_{2h+1}})^n (t_{c_{2h+1}} \cdots t_{c_2} t_{c_1})^n. \end{aligned}$$

The first equivalence follows from repeated use of the fact that t_{c_i} commutes with

$$t_{c_1} t_{c_2} \cdots t_{c_{2h+1}} t_{c_{2h+1}} \cdots t_{c_2} t_{c_1}$$

for all i , which is used to move the underlined term to the left. The second equivalence is the inductive hypothesis. \square

Lemma 1 implies that $H_h(r)$ is equivalent to the Lefschetz fibration with factorization

$$(t_{c_1} t_{c_2} \cdots t_{c_{2h+1}})^{2r} (t_{c_{2h+1}} \cdots t_{c_2} t_{c_1})^{2r}.$$

To depict $H_h(r)$ as a 2-fold branched cover of a Hirzebruch surface using this factorization, we must understand the projection of this factorization to an element of $\text{Mod}(\Sigma_{0,2h+2})$. As before, let D_{2h+2}^2 be a disk that contains all of the marked points, and let $*$ be another marked point in the complement of D_{2h+2}^2 . Using the Alexander method (see [10]), the following is shown in [14].

LEMMA 2. *For all $1 \leq r \leq h$, $(\sigma_1 \cdots \sigma_{2h+1})^{2r} (\sigma_{2h+1} \cdots \sigma_1)^{2r}$ is isotopic to the identity on $\Sigma_{0,2h+2}$ by an isotopy that moves $*$ along a path that passes once between the $(2r)$ th and $(2r+1)$ st marked points without twisting its neighborhood.*

As a result, we see that $H_h(r)$ is the 2-fold branched cover of $S^2 \times S^2$ branched over the ribbon surface shown in Figure 5. The boxed ribbon B_{2r} is defined in the previous

Figure 4.

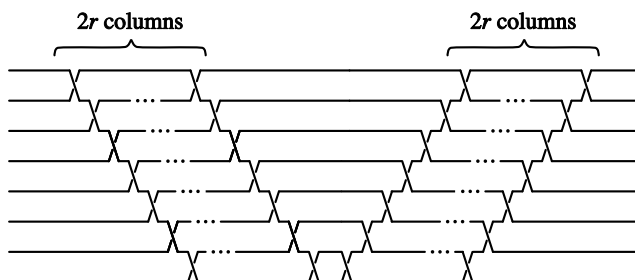


Figure 4. The ribbon surface B_{2r} is obtained by attaching half-twisted bands to parallel disks as shown.

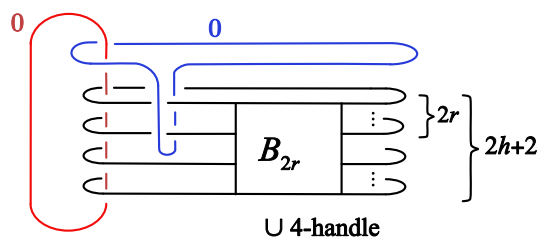


Figure 5. The 2-fold branched cover is $H_h(r)$.

2.3. More Fiber Sums

We can also consider fiber sums between the fibrations on Z_h and H_h . The following proposition is due to Hisaaki Endo.

PROPOSITION 3 ([8], LEMMA 4.1). *The fiber sums $Z_h(2)$ and $H_h(h+1)$ are isomorphic as Lefschetz fibrations.*

As a result, fiber sums between any number of copies of Z_h and H_h are isomorphic to either $H_h(m)$ or $Z_h(1) \#_f H_h(m-1)$, for some m . In both cases, the result is spin if and only if h is odd and m is even [9].

3. The manifolds $X'_{g,h}[i]$

We next derive as Theorem 5 below a relation in the mapping class group $\text{Mod}(\Sigma_g^2)$ which will be used to construct symplectic Lefschetz pencils. This relation, and the corresponding pencils, are a direct generalization of the relations derived in [5]. Instead of adapting the algebraic derivation there, we will proceed by finding a relation in the braid group $\text{Mod}(\Sigma_{0,2g+2}^1)$, which is lifted to a relation in $\text{Mod}(\Sigma_g^2)$ using a 2-fold branched cover. We begin with a Lemma due to Kenneth Chakiris ([6], Lemma 3.5.)

LEMMA 4 (THE REVERSING LEMMA). *Let $\sigma_1, \dots, \sigma_{2g+1}$ be the standard generators of $\text{Mod}(\Sigma_{0,2g+2}^1)$. For any $2 \leq m \leq 2g+1$, we have $(\sigma_1 \cdots \sigma_m)^{m+1} = (\sigma_m \cdots \sigma_1)^{m+1}$.*

Let $1 \leq h < g$. For all $1 \leq j \leq 2g - 2h$, let d_j and e_j denote the curves on Σ_g^2 shown in Figure 6. We abbreviate $D_{2h+2} = t_{d_1} t_{d_2} \cdots t_{d_{2g-2h}}$ and $E_{2h+2} = t_{e_{2g-2h}} \cdots t_{e_2} t_{e_1}$.

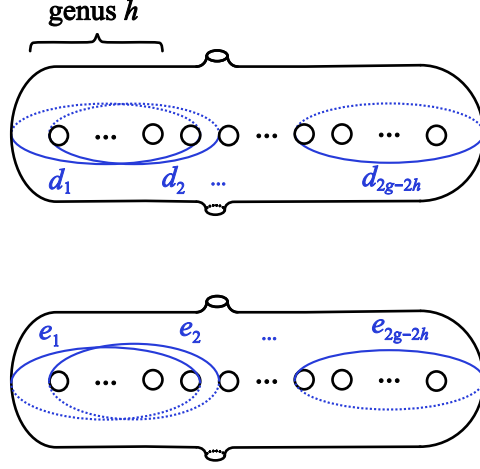


Figure 6. The surface Σ_g^2

THEOREM 5. *Let $1 \leq h < g$, and write $2g + 2$ as $2g + 2 = p(2h + 2) + 2r$, with $p > 0$ and $0 \leq r < h + 1$. Then in $\text{Mod}(\Sigma_g^2)$ we have*

$$t_\delta t_{\delta'} = D_{2h+2} E_{2h+2} (t_{c_1} \cdots t_{c_{2h+1}})^{(2h+2)(2p-1)} (t_{c_{2h+3}} \cdots t_{c_{2g+1}})^{2g-2h} (t_{c_1} \cdots t_{c_{2h+1}})^{2r} (t_{c_{2h+1}} \cdots t_{c_1})^{2r},$$

where δ and δ' are curves parallel to the boundary components of Σ_g^2 .

REMARK. When $r = 0$, the terms $(t_{c_1} \cdots t_{c_{2h+1}})^{2r} (t_{c_{2h+1}} \cdots t_{c_1})^{2r}$ are omitted from the factorization.

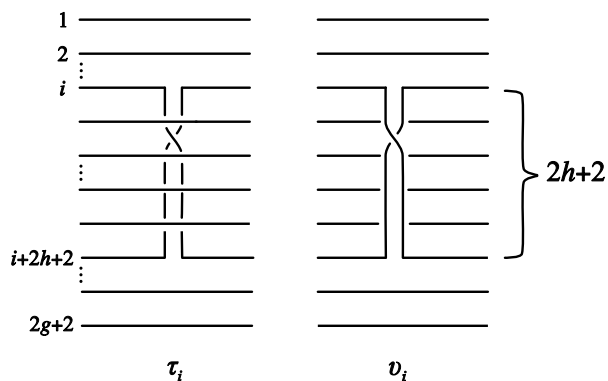
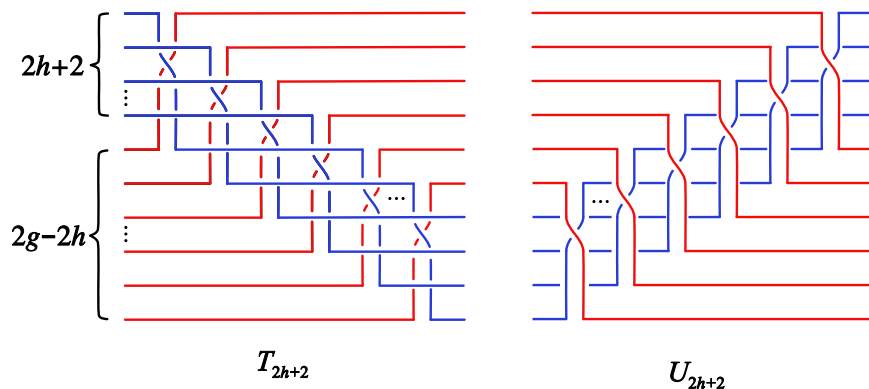
PROOF. We give a proof using braids, in the spirit of Lemma 8 of [1], by identifying the classical braid group on $2g + 2$ strands with the mapping class group $\text{Mod}(\Sigma_{0,2g+2}^1)$ of the disk with $2g + 2$ marked points. Define τ_i and v_i to be the braids shown in Figure 7.

Consider $T_{2h+2} = \tau_1 \tau_2 \cdots \tau_{2g-2h}$ and $U_{2h+2} = v_{2g-2h} \cdots v_2 v_1$, shown in Figure 8. It is easy to see that T_{2h+2} passes the upper $2h + 2$ strands over the lower $2g - 2h$ strands, forming a right half twist between the two collections. The upper strands, regarded by themselves, form the braid $(\bar{\sigma}_1 \cdots \bar{\sigma}_{2h+1})^{2g-2h}$, while the lower strands are parallel. Similarly, for U_{2h+2} , the upper $2g - 2h$ strands pass over the lower $2h + 2$ strands, forming a right half twist between the two collections. The lower strands, regarded by themselves, form the braid $(\bar{\sigma}_{2h+1} \cdots \bar{\sigma}_1)^{2g-2h}$, with the upper strands parallel.

Adding additional generators to the product $T_{2h+2} U_{2h+2}$, we claim that

$$T_{2h+2} U_{2h+2} (\sigma_1 \cdots \sigma_{2h+1})^{2g-2h} (\sigma_{2h+1} \cdots \sigma_1)^{2g+2} (\sigma_{2h+3} \cdots \sigma_{2g+1})^{2g-2h}$$

forms a full right twist among all strands.


 Figure 7. The braids τ_i and ν_i

 Figure 8. The braids T_{2h+2} and U_{2h+2}

This can be seen by expanding this expression as:

$$T_{2h+2}U_{2h+2}(\sigma_1 \cdots \sigma_{2h+1})^{2g-2h}(\sigma_{2h+1} \cdots \sigma_1)^{2g-2h}(\sigma_{2h+1} \cdots \sigma_1)^{2h+2}(\sigma_{2h+3} \cdots \sigma_{2g+1})^{2g-2h}.$$

The additional terms

$$(\sigma_1 \cdots \sigma_{2h+1})^{2g-2h}(\sigma_{2h+1} \cdots \sigma_1)^{2g-2h}$$

following $T_{2h+2}U_{2h+2}$ undo the braiding among the upper $2h+2$ strands, and the subsequent terms

$$(\sigma_{2h+1} \cdots \sigma_1)^{2h+2}(\sigma_{2h+3} \cdots \sigma_{2g+1})^{2g-2h}$$

separately introduce a full right twist within both the upper $2h+2$ and lower $2g-2h$ strands. This results in a full right twist among *all* strands, as claimed.

The assumed condition $2g+2 = p(2h+2) + 2r$ implies $2g-2h = (p-1)(2h+2) + 2r$.

Substituting both and using the Reversing Lemma we get

$$\begin{aligned}
& T_{2h+2}U_{2h+2}(\sigma_1 \cdots \sigma_{2h+1})^{2g-2h}(\sigma_{2h+1} \cdots \sigma_1)^{2g+2}(\sigma_{2h+3} \cdots \sigma_{2g+1})^{2g-2h} \\
&= T_{2h+2}U_{2h+2}(\sigma_1 \cdots \sigma_{2h+1})^{(2h+2)(p-1)+2r}(\sigma_{2h+1} \cdots \sigma_1)^{(2h+2)p+2r}(\sigma_{2h+3} \cdots \sigma_{2g+1})^{2g-2h} \\
&= T_{2h+2}U_{2h+2}(\sigma_1 \cdots \sigma_{2h+1})^{(2h+2)(2p-1)}(\sigma_1 \cdots \sigma_{2h+1})^{2r}(\sigma_{2h+1} \cdots \sigma_1)^{2r} \\
&\hspace{20em}(\sigma_{2h+3} \cdots \sigma_{2g+1})^{2g-2h}.
\end{aligned}$$

(Note that if $r = 0$, the terms with exponent $2r$ become unnecessary.)

Since this braid is a full right twist, interpreting the braid as an element of the mapping class group $\text{Mod}(\Sigma_{0,2g+2}^1)$ of the disk with $2g+2$ marked points, this expression is in the same class as a Dehn twist about a curve parallel to the boundary ([10]). The result follows by lifting this relation under the 2-fold branched cover $\Sigma_g^2 \rightarrow \Sigma_{0,2g+2}^1$ with $2g+2$ branch points; the lifts of T_{2h+2} and U_{2h+2} are D_{2h+2} and E_{2h+2} , respectively, and each σ_i lifts to t_{c_i} . \square

Starting from the factorization in Theorem 5, for any $0 \leq i \leq 2p-1$ we can perform i unchaining surgeries to the subword $(t_{c_1}t_{c_2} \cdots t_{c_{2h+1}})^{2h+2}$, and another one to the subword $(t_{c_{2h+3}} \cdots t_{c_{2g+1}})^{2g-2h}$. This yields the relation

$$D_{2h+2}E_{2h+2}t_a^i t_{a'}^i t_b t_{b'} (t_{c_1} \cdots t_{c_{2h+1}})^{(2h+2)(2p-1-i)} (t_{c_1} \cdots t_{c_{2h+1}})^{2r} (t_{c_{2h+1}} \cdots t_{c_1})^{2r} = t_\delta t_{\delta'}$$

in $\text{Mod}(\Sigma_g^2)$, where a, a', b, b' are shown in Figure 9.

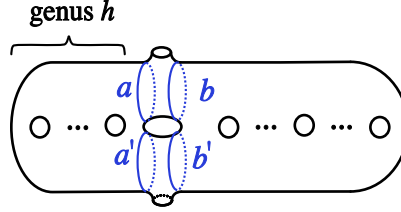


Figure 9. The curves a, a', b, b' on Σ_g^2

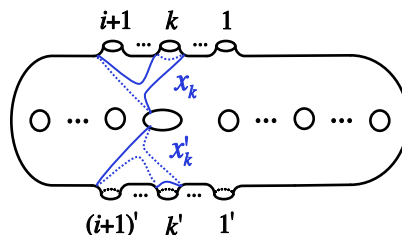
The clever inductive argument using the lantern relation found in the proof of Theorem 4.6 of [5] can now be applied verbatim to lift this relation to $\text{Mod}(\Sigma_g^{2(i+1)})$ as

$$(1) \quad \Delta = D_{2h+2}E_{2h+2}(t_{x_1}t_{x_2} \cdots t_{x_{i+1}})(t_{x'_1}t_{x'_2} \cdots t_{x'_{i+1}})(t_{c_1}t_{c_2} \cdots t_{c_{2h+1}})^{(2h+2)(2p-i-1)} \\
(t_{c_1}t_{c_2} \cdots t_{c_{2h+1}})^{2r}(t_{c_{2h+1}} \cdots t_{c_2}t_{c_1})^{2r},$$

where Δ is the product of right-handed Dehn twists about a curve parallel to each boundary component of $\Sigma_g^{2(i+1)}$. The curves x_k and x'_k are shown in Figure 10.

This factorization gives the following theorem.

THEOREM 6. *Let $1 \leq h < g$, and write $2g+2$ as $2g+2 = p(2h+2) + 2r$, with $p > 0$ and $0 \leq r < g+1$. Then for all $0 \leq i \leq 2p-1$, there is a symplectic 4-manifold $X'_{g,h}[i]$ which admits a genus g Lefschetz pencil with monodromy factorization in $\text{Mod}(\Sigma_g^{2(i+1)})$*


 Figure 10. The curves x_k, x'_k on $\Sigma_g^{2(i+1)}$

given by Equation (1).

REMARK. Setting $h = 1$ in Equation (1) reproduces Baykur-Hayano-Monden's relations in Theorem 4.6 of [5] and consequently their manifolds correspond to our manifolds $X'_{g,1}[i]$. In their description, separate factorizations are given for g even and odd. Thus Theorem 5 simultaneously consolidates their factorization into a single statement for both cases while also generalizing it to hold for all h .

PROPOSITION 7. *The manifolds $X'_{g,h}[i]$ have Euler characteristic*

$$e(X'_{g,h}[i]) = 4 - 4h + 2(2h + 1)(2g + 2) - (i + 1)(2h + 1)(2h + 2)$$

and signature

$$\sigma(X'_{g,h}[i]) = -(2h + 2)(2g + 2) + 2(i + 1)(h + 1)^2.$$

PROOF. These formulas can be seen in several ways, and we leave the details to the reader. For instance, the Euler characteristic follows from translating the factorization in Equation (1) into the standard handlebody description of the Lefschetz fibration $X_{g,h}[i]$ obtained by blowing up $X'_{g,h}[i]$. The signature can be seen by using Endo's fractional signature to first compute the signature of the Lefschetz fibration defined by the factorization in Theorem 5 (see [7]), and then using Endo and Nagami's results from [9] to obtain the signature of manifolds obtained by unchaining surgery. Both formulas can also be corroborated using the branched covering description of $X'_{g,h}[i]$ developed in the next section. \square

PROPOSITION 8. *Let $1 \leq h < g$, and write $2g + 2$ as $2g + 2 = p(2h + 2) + 2r$, with $p > 0$ and $0 \leq r < g + 1$. Suppose either $0 \leq i < 2p - 1$; or, $i = 2p - 1$ and $r > 1$. Then $X'_{g,h}[i]$ is simply connected, and is neither rational nor ruled.*

PROOF. It is straightforward to use the monodromy factorization in Equation (1) to determine that the fundamental group of $X'_{g,h}[i]$ is trivial. Alternately, this also follows from the proof of Theorem 9 below, which displays $X_{g,h}[i]$ as a blow up of a simply connected manifold. Thus $X'_{g,h}[i]$ ruled is ruled out.

Knowing $b_1(X'_{g,h}[i]) = 0$, the formulas in Proposition 7 imply that

$$b_2^+(X'_{g,h}[i]) = 1 + h[(2g + 2) - (i + 1)(h + 1) - 2].$$

Substituting the factorization $2g + 2 = p(2h + 2) + 2r$ and simplifying gives

$$b_2^+(X'_{g,h}[i]) = 1 + h[(h + 1)(2p - 1 - i) + 2(r - 1)].$$

The conditions on i and r imply that $b_2^+(X'_{g,h}[i]) > 1$, and so $X'_{g,h}[i]$ is not rational. \square

REMARK. At this point, we may also use the monodromy factorization in Equation (1) to state conditions on g, h , and i that determine when $X'_{g,h}[i]$ is spin, using the technique developed in [5]. However, this also follows easily from our Theorem 9 below, and we defer this statement to Corollary 10.

3.1. A branched cover description of $X'_{g,h}[i]$

We now describe the manifolds $X'_{g,h}[i]$ as 2-fold branched covers of a rational surface. Let \mathbb{F}_n denote the n th Hirzebruch surface. We assume throughout this section that either $0 \leq i < 2p - 1$; or, $i = 2p - 1$ and $r > 1$.

We begin by considering the Lefschetz fibration $X_{g,h}[i]$ obtained by blowing up the pencil on $X'_{g,h}[i]$ at its base points. Under the capping homomorphism $\text{Mod}(\Sigma_g^{2(i+1)}) \rightarrow \text{Mod}(\Sigma_g)$, the various curves x_k and x'_k in Figure 10 become a common curve x and x' and we have that

$$D_{2h+2}E_{2h+2}t_x^{i+1}t_{x'}^{i+1}(t_{c_1}t_{c_2}\cdots t_{c_{2h+1}})^{(2h+2)(2p-i-1)}(t_{c_1}t_{c_2}\cdots t_{c_{2h+1}})^{2r}(t_{c_{2h+1}}\cdots t_{c_2}t_{c_1})^{2r}$$

is the identity in $\text{Mod}(\Sigma_g)$. From this relation, we express $X_{g,h}[i]$ as the 2-fold cover of $\mathbb{F}_1 \# (i + 1)\overline{\mathbb{C}\mathbb{P}^2}$ branched over the surface shown in Figure 11. In this diagram, A_{2g+2} represents the ribbon surface bounded by the braid $T_{2h+2}U_{2h+2}$ as shown in Figure 8. The exponent of $(C_{2h+2})^{2p-i-1}$ denotes multiple copies of the ribbon surface C_{2h+2} . The collection of -1 -framed 2-handles linking the ribbon surface each lift to a pair of 2-handles corresponding to a pair of Dehn twists t_x and $t_{x'}$ in the monodromy factorization for $X_{g,h}[i]$. The other terms in the factorization correspond to 2-handles that are lifts of bands in the various ribbon surfaces pictured. The -1 -framed 2-handle that is a meridian to the 0-framed one appears as shown because the projection of the monodromy to $\Sigma_{0,2g+2}$ equals a single right-handed Dehn twist about all branch points; this fact follows from its derivation in Theorem 5, and is also confirmed with the Alexander method in [16]. The branch surface includes $2g + 2$ disks in the 4-handle attached to the boundary of the ribbon surface pictured.

We next modify the base of this branched covering, for use in the next section. We begin by repositioning the -1 -framed 2-handles that link the ribbon surface by moving them to the right and swinging them around the back of the ribbon surface so that they appear on the left, as shown in Figure 12.

We now slide one of the upper -1 -framed 2-handle over the lower one, giving Figure 13. Figures 13 through 15 then show a sequence of handle slides, indicated by the bands in each picture. The steps from Figure 12 to 15 can then be repeated for each of the $i - 1$ many -1 -framed 2-handles at the top of Figure 12, resulting in Figure 16. Two more handle slides bring us to Figure 18.

We blow down each of the exceptional spheres in Figure 18 given by the -1 -framed 2-handles to arrive at Figure 19. We claim that the 2-fold branched cover of \mathbb{F}_{i+1} branched over the surface pictured in Figure 19 is $X'_{g,h}[i]$. We note first that lifts of each of the

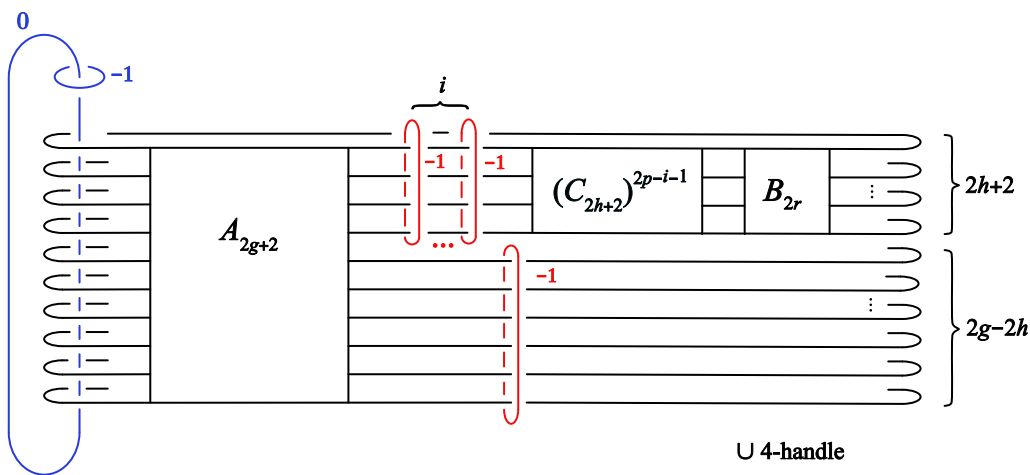


Figure 11. The 2-fold branched cover is $X_{g,h}[i]$.

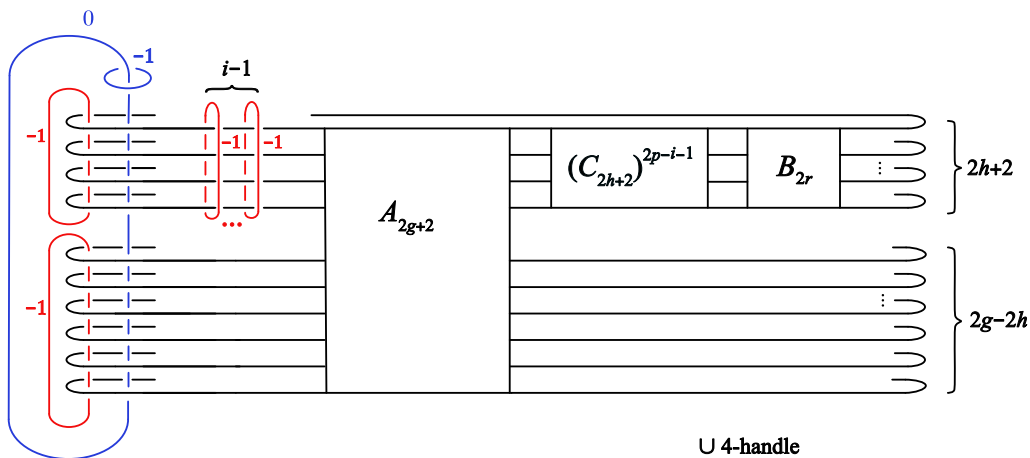


Figure 12.

exceptional spheres in Figure 18 are sections of the fibration on $X_{g,h}[i]$. This can be seen by observing that the 0-framed 2-handle is fixed by the diffeomorphism that is the transition from Figure 12 to Figure 18. These spheres are -1 -framed meridians to this 2-handle in Figure 18, and thus when those spheres are traced back to Figure 12 they lift to two sections of the fibration on $X_{g,h}[i]$ of square -1 . It is not directly apparent that these sections correspond to those obtained from blowing up the pencil on $X'_{g,h}[i]$. However, we will see in Section 4.2 – independently of this claim – that the 2-fold cover in Figure 19 is minimal. Since Proposition 8 implies that $X_{g,h}[i]$ is neither rational nor ruled, it follows from Corollary 3 of [18] that this cover is diffeomorphic to $X'_{g,h}[i]$, as claimed.

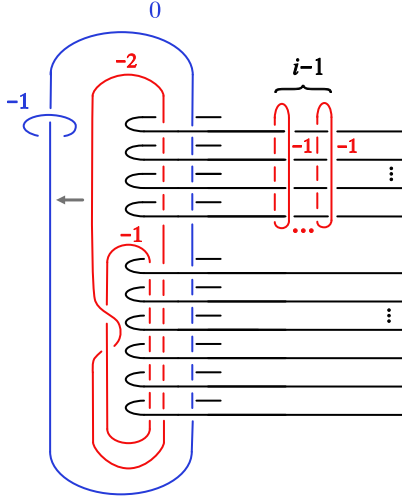


Figure 13.

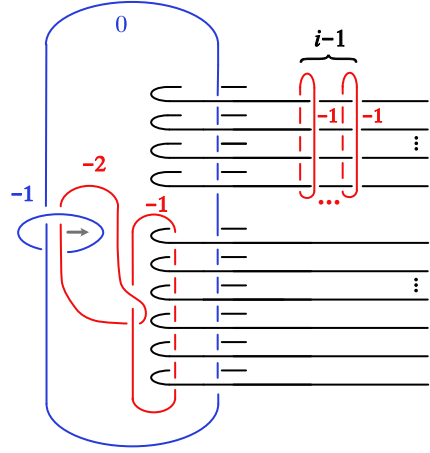


Figure 14.

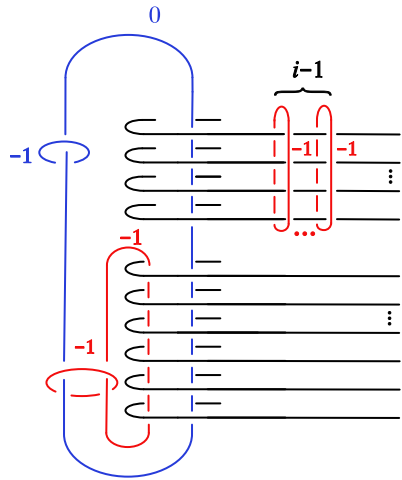


Figure 15.

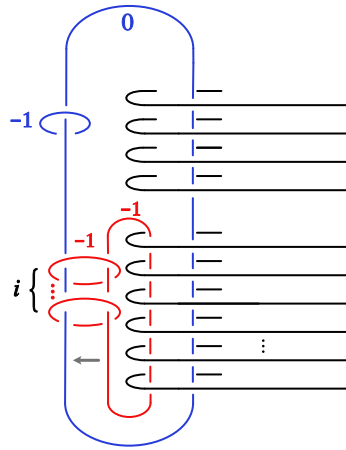


Figure 16.

4. From pencils to fibrations

We are now ready for our main theorem, which identifies the manifolds $X'_{g,h}[i]$ as complex manifolds obtained as fiber sums of the genus h Lefschetz fibrations from Section 2.

THEOREM 9. *Let $1 \leq h < g$, and write $2g+2$ as $2g+2 = p(2h+2) + 2r$, with $p > 0$ and $0 \leq r < h+1$.*

- (a) *For all $0 \leq i < 2p-1$, $X'_{g,h}[i]$ is diffeomorphic to $Z_h(2p-1-i) \#_f H_h(r)$. If $r=0$, then $H_h(r)$ is omitted from this expression.*
- (b) *If $i = 2p-1$ and $r > 1$, then $X'_{g,h}[2p-1]$ is diffeomorphic to $H_h(r)$.*

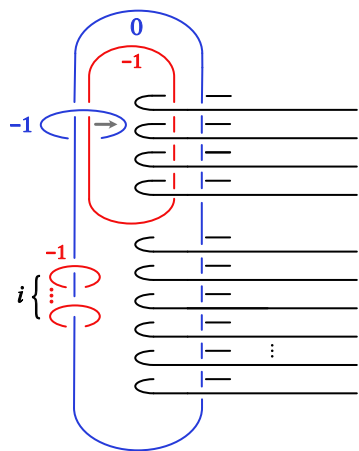


Figure 17.

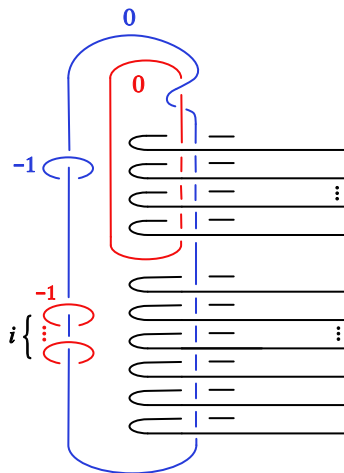


Figure 18.

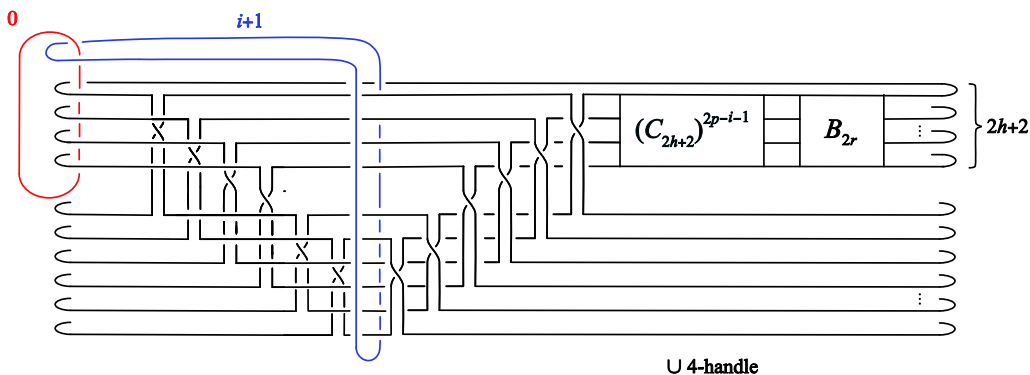


Figure 19. The 2-fold branched cover is $X'_{g,h}[i]$.

Before addressing the proof of Theorem 9, we record two corollaries.

COROLLARY 10. *Assume $0 \leq i < 2p - 1$; or, $i = 2p - 1$ and $r > 1$. Then $X'_{g,h}[i]$ is spin if and only if h is odd and g and i have the same parity.*

PROOF. Recall that any fiber sum involving Z_h and H_h is equivalent to one of $Z_h(1) \#_f H_h(m - 1)$ or $H_h(m)$, with the result spin if and only if h is odd and m is even ([9]).

Assume for the rest of the proof that h is odd. Dividing the equation $2g + 2 = p(2h + 2) + 2r$ by 2 shows that under this assumption, g and r always have opposite parity.

Assume i is odd. Then Proposition 3 implies that $Z_h(2p - 1 - i) \#_f H_h(r)$ is equivalent to

$$H_h\left(\left(p - \frac{i+1}{2}\right)(h + 1) + r\right).$$

This is spin if and only if the expression $(p - \frac{i+1}{2})(h+1) + r$ is even. This happens if and only if r is even, or equivalently if and only if g is odd.

Assume i is even. Then Proposition 3 implies that $Z_h(2p-1-i) \#_f H_h(r)$ is equivalent to

$$Z_h(1) \#_f H_h((p - \frac{i+2}{2})(h+1) + r).$$

This is spin if and only if the expression $(p - \frac{i+2}{2})(h+1) + r$ is odd. This happens if and only if r is odd, or equivalently if and only if g is even. \square

By regarding g and i in the expressions in Theorem 9 as functions of p , we see that any given fiber sum with summands Z_h and H_h admits infinitely many Lefschetz pencils, whose genera grow without bound as an arithmetic sequence. To state this in general, observe that by Proposition 3, for $h \geq 2$ any such fiber sum can be uniquely expressed as $Z_h(q) \#_f H_h(r)$, for some $0 \leq r < h+1$ and $q \geq 0$. Equating the number of Z_h summands with the expression in Theorem 9 gives $q = 2p - i - 1$, or $i = 2p - 1 - q$. The expression $2g + 2 = p(2h + 2) + 2r$ simplifies to $g = p(h + 1) + r - 1$. Thus we have

COROLLARY 11. *Let $h \geq 1$. Assume $0 \leq r < h + 1$ and $q \geq 0$. Set $g(p) = p(h + 1) + r - 1$ and $i(p) = 2p - 1 - q$. Then $Z_h(q) \#_f H_h(r)$ is diffeomorphic to $X'_{g(p),h}[i(p)]$ for all $p \geq \max\{\frac{1}{2}(q + 1), 2\}$.*

REMARK. The condition $p \geq \max\{\frac{1}{2}(q + 1), 2\}$ guarantees that $i \geq 0$ and $g > h$ for all p .

4.1. An isotopy lemma

To prove Theorem 9, we start with a lemma which describes an isotopy between two ribbon surfaces embedded in a Hirzebruch surface. The surfaces are given by banded unlink diagrams, and the isotopy makes use of some standard moves on these diagrams, a complete list of which is given in [17]. We will make use of two iterations of these moves, previously described in [13], where they were referred to as *band dives* and *2-handle band dives*, respectively. These moves are summarized in Figures 20 and 21; they will be used by replacing the initial ribbon surface in each figure with the final one.

Let $\Sigma(R, S, T)$ denote a ribbon surface in the n th Hirzebruch surface \mathbb{F}_n of the form shown in Figure 22. The “length” of each long band in the surface is a fixed constant k , which we suppress from the notation. The box represents any collection of bands subject to the requirement that they are confined to that region. The parameters R, S and T are explained in the caption to Figure 22.

LEMMA 12 (THE ISOTOPY LEMMA). *Let $k \geq 2$. For any $R \geq 2k$, the ribbon surface $\Sigma(R, S, T)$ is isotopic to the ribbon surface $\Sigma(R - k, S + 1, T + k)$.*

PROOF. The strategy of the proof is to use the long bands on the left side of Figure 22 – the ones that pass inside the horizontal disks – to cancel the lower horizontal disks. To do so, we must first move the n -framed attaching circle and the outside long bands out of the way.

To execute this strategy, we use a 2-handle band dive to arrive at Figure 23. Note that S changes to $S + 1$. We next use a band slide to obtain Figure 24, followed by a

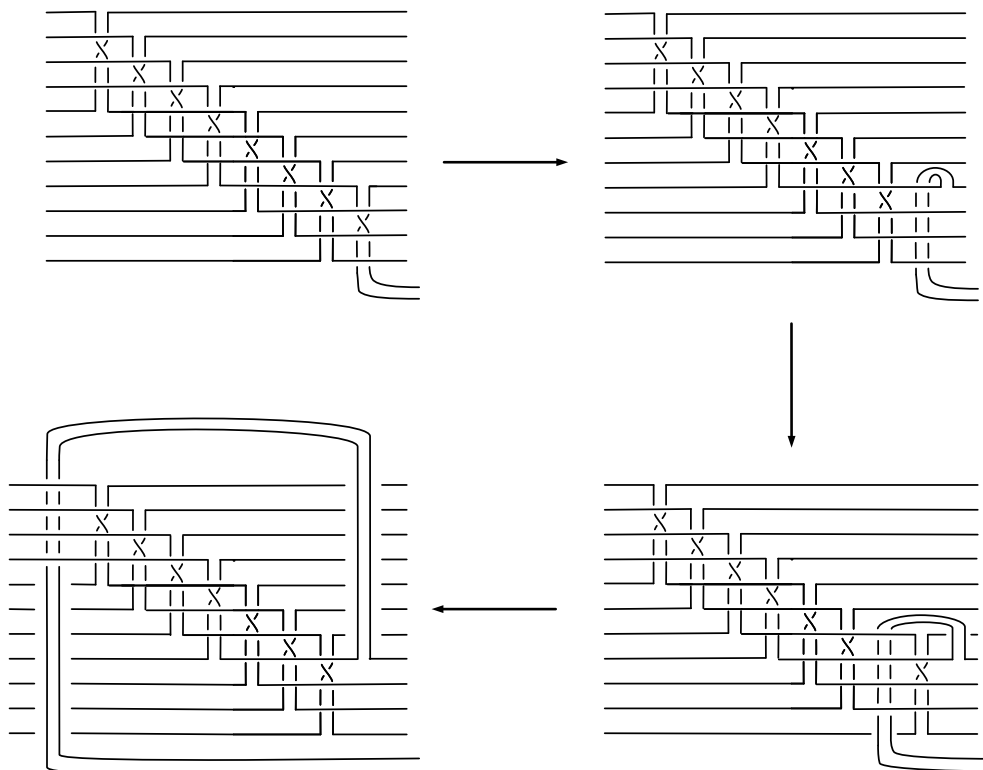


Figure 20. A band dive

band dive to arrive at Figure 25.

A 2-handle band slide over the 0-framed 2-handle, using the indicated band untangles the band from the upper k horizontal disks, after which it is isotoped to the location shown in Figure 26. This figure also shows one fewer horizontal disk, as we are now able to cancel the bottommost disk in Figure 25 with the remaining attached band.

We now repeat the steps between Figure 23 and Figure 26 $k - 1$ times, cancelling $k - 1$ more horizontal disks while adding $k - 1$ more trivial bands. The outcome is shown in Figure 27. (We have also slid all of the newly introduced trivial bands to the upper k rows of disks.) Altogether, the triple (R, S, T) has been replaced by the triple $(R - k, S + 1, T + k)$, proving the Lemma. \square

4.2. Proof of Theorem 9

Observe that in the notation of the Isotopy Lemma of Section 4.1, the branch surface in Figure 19 is of the form $\Sigma(2g + 2, 0, 0)$, with $k = 2h + 2$. Applying the Isotopy Lemma $p - 1$ times gives that $X'_{g,h}[i]$ is the 2-fold branched cover of \mathbb{F}_{i+1} branched over $\Sigma(2h + 2 + r, p - 1, (p - 1)(2h + 2))$, as seen in Figure 28.

We continue the process to cancel the bottom r horizontal disks. If $r = 0$, these disks and the long bands are not there, and these steps are unnecessary. Otherwise, a 2-handle band dive results in Figure 29. We then iterate r times the moves from Figure 23 to Figure 26 to remove these bottom disks, at the expense of adding r more trivial bands to the branch surface. There are now $(p - 1)(2h + 2) + r = 2g - 2h$ trivial bands in total.

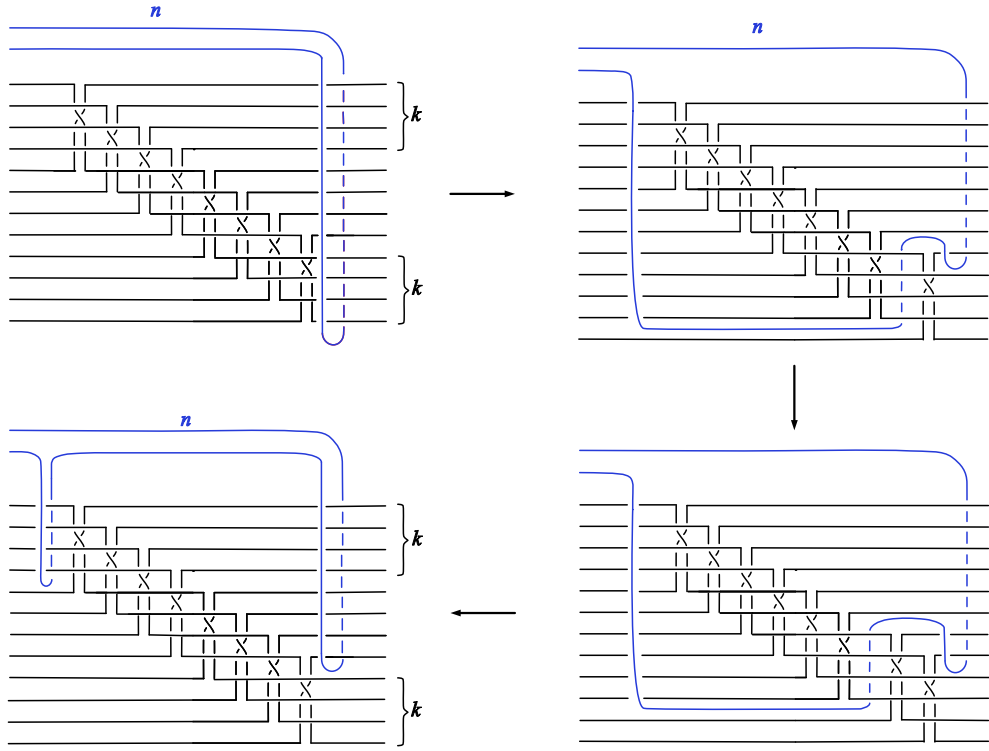


Figure 21. A 2-handle band dive

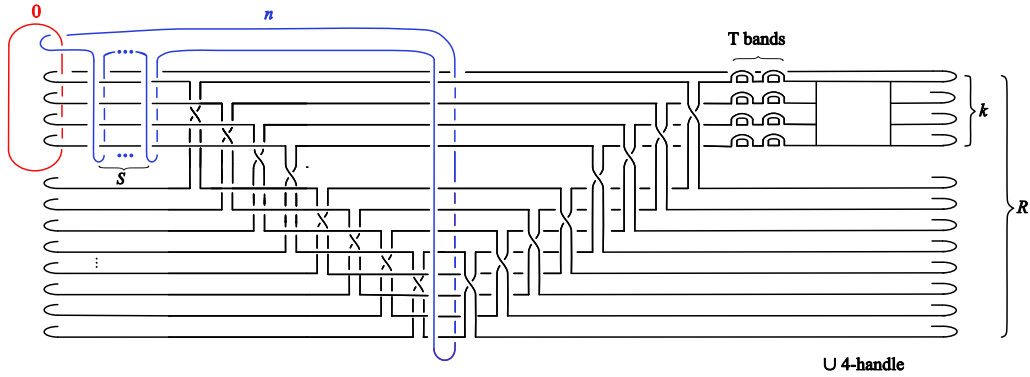


Figure 22. The ribbon surface $\Sigma(R, S, T)$ has R horizontal disks. The n -framed attaching circle links the horizontal disks S times positively in the indicated region. There are T trivial bands attached to the top k horizontal disks.

Cancelling all of them with disks in the 4-handle leaves $2h + 2$ remaining in the 4-handle of the result, shown in Figure 30. Finally we slide the $(i + 1)$ -framed 2-handle p times over the 0-framed handle, resulting in Figure 31.

Comparing Figure 31 with the branched cover descriptions of Z_h and $H_h(r)$ in Figures 3 and 5 shows that the 2-fold branched cover of Figure 31 describes the fiber sum

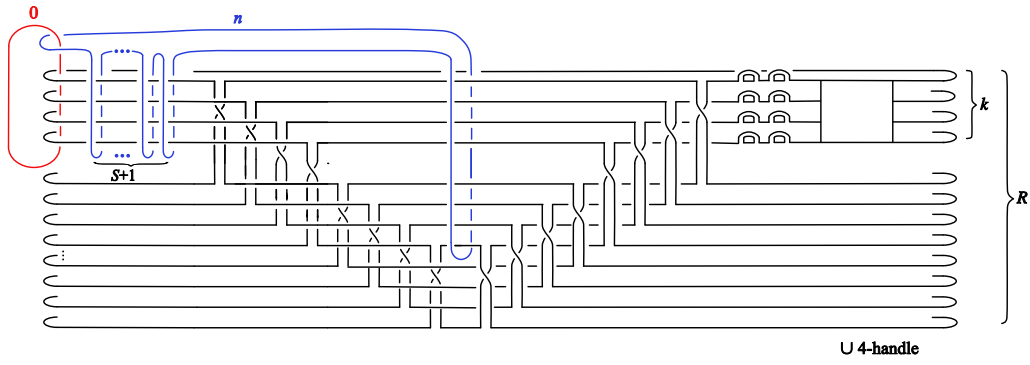


Figure 23.

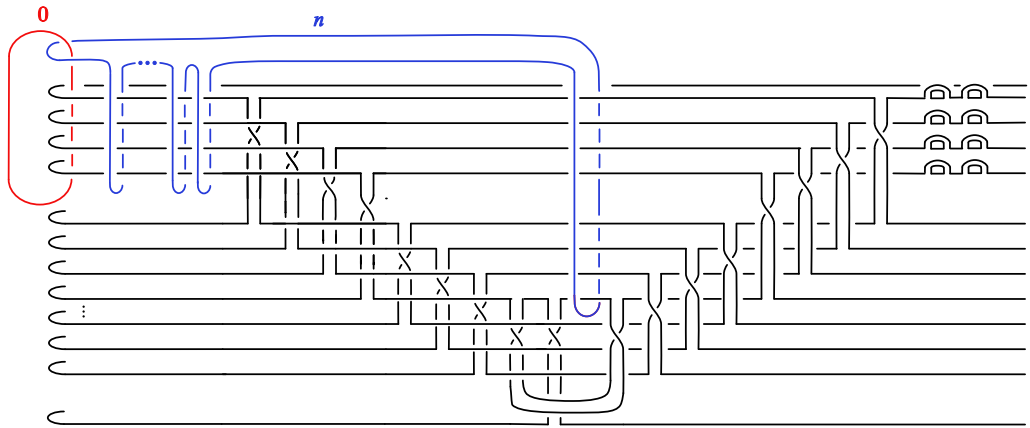


Figure 24.

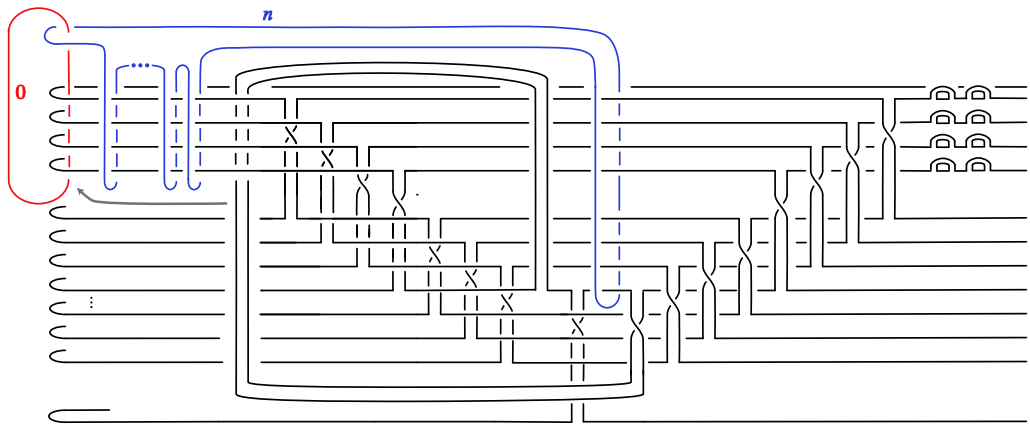


Figure 25.

$$Z_h(2p - 1 - i) \#_f H_h(r).$$

Note that when $i < 2p - 1$ and $r = 0$, the boxed collection of bands B_{2r} is omitted

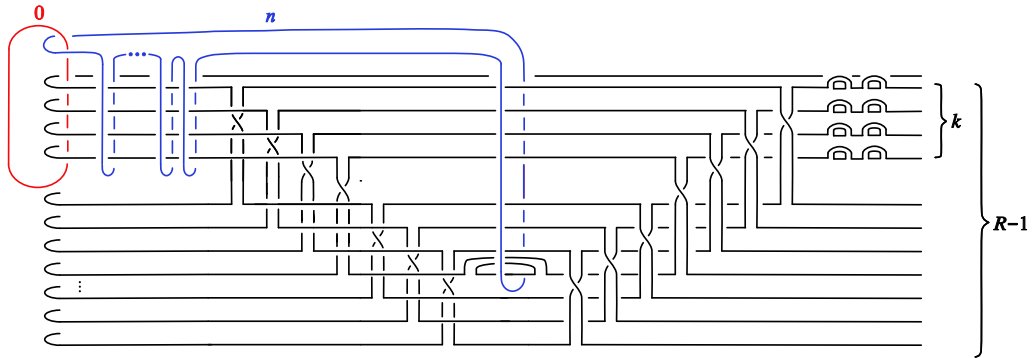


Figure 26.

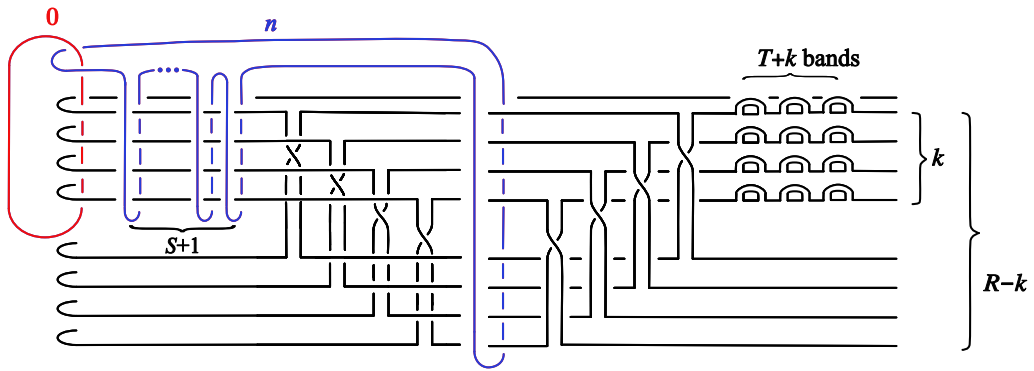


Figure 27.

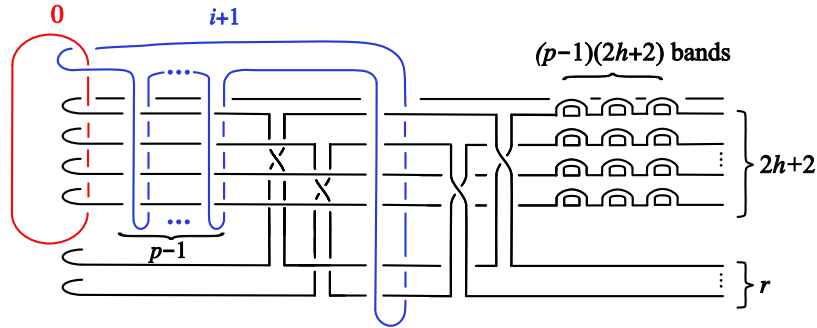


Figure 28.

from the figures. Furthermore, it is straightforward to see that when $r = 0$, omitting the unnecessary steps in the proof will remove the linking of the $-(2p - i - 1)$ -framed 2-handle in Figure 31 with the ribbon surface. Thus in this case, comparing Figure 31 to Figure 3 shows that the 2-fold branched cover is $Z_h(2p - i - 1)$, as claimed. When $i = 2p - 1$, the boxed collection of bands $(C_{2h+2})^{2p-i-1}$ is omitted from the figures, and Figure 31 reduces to Figure 5; the cover is $H_h(r)$, as required. This completes the proof

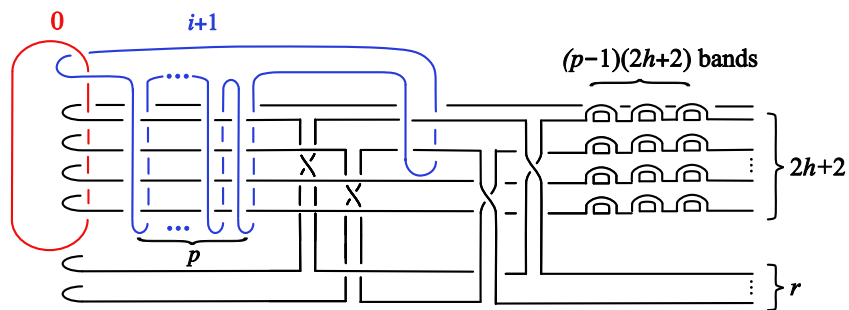


Figure 29.

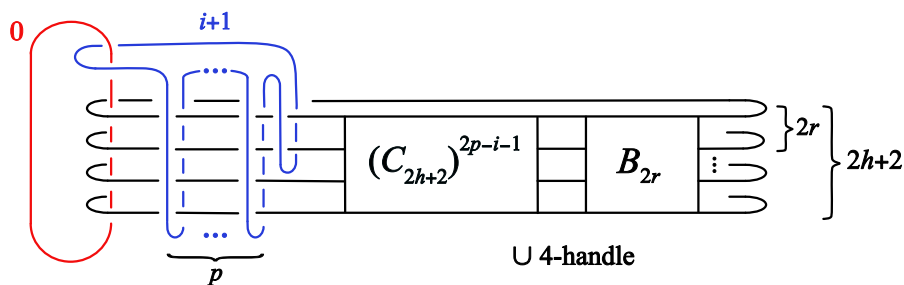


Figure 30.

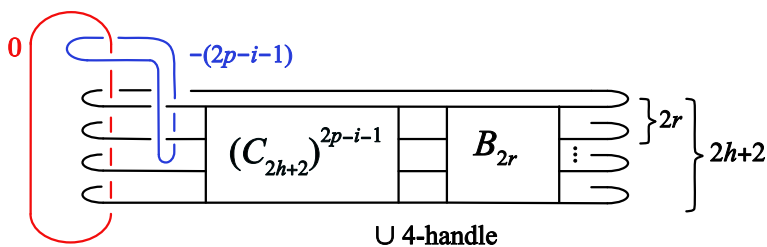


Figure 31. The 2-fold branched cover is $Z_h(2p - 1 - i) \#_f H_h(r)$.

of Theorem 9.

REMARK. The handle calculus and isotopies used in the proof of Theorem 9 also reveal weaker statements about cases not covered by the hypotheses of the theorem. Recall that the assumptions $0 \leq i < 2p - 1$, or $i = 2p - 1$ and $r > 1$, were required to ensure $X'_{g,h}[i]$ is neither rational nor ruled, a necessary requirement for it to be represented as the 2-fold branched cover shown in Figure 19. Nevertheless, the diffeomorphism between the covers of Figures 19 and 31 carries through regardless of these assumptions.

When $i = 2p - 1$ and $r = 1$, Figure 31 reduces to a manifold whose 2-fold branched cover is the rational surface $H_h(1)$. Thus we see that there are $2(i + 1)$ sections of $X_{g,h}[i]$ that can be blown down to yield a pencil on $H_h(1)$, but we cannot conclude that pencil is the one described by the factorization that defines $X'_{g,h}[i]$.

Similarly, when $i = 2p - 1$ and $r = 0$, both boxed collections of bands $(C_{2h+2})^{2p-i-1}$

and B_{2r} are omitted from Figure 19. Then Figure 31 reduces to Figure 32, which describes the cover $\Sigma_h \times S^2 \rightarrow S^2 \times S^2$ obtained as the product of the 2-fold cover $\Sigma_h \rightarrow \Sigma_{0,2h+2}$ with the identity. In this case, there are $2(i+1)$ sections of $X_{g,h}[i]$ that can be blown

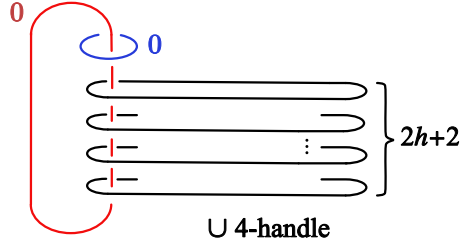


Figure 32. The 2-fold branched cover is $\Sigma_h \times S^2$.

down to yield a pencil on the ruled surface $\Sigma_h \times S^2$, but again we cannot conclude that pencil is the one arising from the factorization that defines $X'_{g,h}[i]$.

5. Remarks

5.1. Degree Doubling

Corollary 11 describes an infinite family of pencils whose fiber genus grows without bound on a fixed symplectic 4-manifold. This invites comparison with *degree doubling*, a construction in which a Donaldson pencil on a symplectic (X, ω) with fiber class Poincaré dual to $d[\omega]$ gives rise to a higher genus pencil on X with fiber class dual to $2d[\omega]$. This operation was studied by Ivan Smith in [23], and by Denis Auroux and Ludmil Katzarkov for pencils described as branched covers of $\mathbb{C}P^2$ in [3]. Degree doubling was later shown by Baykur to be an operation applicable to any topological genus g Lefschetz pencil, provided the number of base points does not exceed $2g - 2$ ([4]).

It is clear that on a given genus h hyperelliptic Lefschetz fibration, the pencils produced by Corollary 11 are more abundant than those generated by degree doubling, as their genus grows according to an arithmetic sequence (with common difference $h + 1$), whereas doubling increases genus exponentially. One may still wonder if pencils generated by doubling occur as a subsequence of our construction. A simple observation shows that this is not the case. In degree doubling, a Lefschetz pencil of genus g with b base points is doubled to become a pencil of genus $g' = 2g + b - 1$ with $b' = 4b$ base points. In particular, the resulting number of base points is always a multiple of 4. However, this does not hold for some families of pencils described by Corollary 11: for instance, $Z_2(1)$ is diffeomorphic to each pencil in the sequence $X'_{3p-1,2}[2p-2]$ for $p \geq 2$, which have $2(i+1) = 2(2p-1) = 4p-2$ base points, a number never divisible by 4.

5.2. Horikawa surfaces

The even chain relation $(t_{c_1}t_{c_2}t_{c_3}t_{c_4})^{10} = 1$ in $\text{Mod}(\Sigma_2)$ corresponds to a genus 2 Lefschetz fibration on a complex surface Y_2 . The manifolds Y_2, H_2 , and Z_2 , as well as their fiber sums, all obey the Noether inequality (see [15]), making them examples of complex manifolds known as *Horikawa surfaces*. For $\ell \geq 3$ and odd, the fiber sums $H_2(2\ell)$ and $Y_2(\ell)$ are homeomorphic, and it remains a long standing open question to

determine whether they are diffeomorphic and/or symplectomorphic. (For ℓ even they are not homeomorphic. For $\ell = 1$, they are homeomorphic but not diffeomorphic [11].)

In [2], Auroux derived explicit monodromy factorizations for the canonical Lefschetz pencils on both $H_2(6)$ and $Y_2(3)$. Each was seen to be a genus 17 pencil with 16 base points and 196 nodal fibers, and Auroux shows that in fact they are related by a partial twisting operation (or, equivalently, by a Luttinger surgery). Moreover, the corresponding monodromy groups are isomorphic, in contrast to the monodromy groups of the genus 2 fibrations on these manifolds.

By Corollary 11, we see that $H_2(6)$ is diffeomorphic to $X'_{17,2}$ [7] constructed here, which is also a genus 17 pencil with 16 base points and 196 nodes. The factorization for Auroux's pencil ([2], Theorem 4.4) appears quite a bit different from that in our Theorem 6 (with $g = 17, h = 2, i = 7$). It is an interesting question to determine if these genus 17 pencils on $H_2(6)$ are Hurwitz equivalent. Moreover, the infinite family of Lefschetz pencils on $H_2(6)$ derived from Corollary 11 includes some of lower genus, namely $X'_{8,2}$ [1], $X'_{11,2}$ [3] and $X'_{14,2}$ [5]. These “smaller” pencils may prove useful in studying the differential topology of $H_2(6)$.

Finally, we speculate that there may be a result similar to Theorem 9 which constructs families of Lefschetz pencils on manifolds defined from the hyperelliptic Lefschetz fibration corresponding to the even chain relation in $\text{Mod}(\Sigma_h)$. Such a result would provide pencils which could be compared to Auroux's canonical pencil on $Y_2(3)$ ([2], Theorem 3.2), and may also supply new smaller genus pencils on that manifold.

References

- [1] D. Auroux, *A stable classification of Lefschetz fibrations*, *Geom. Topol.* **9** (2005) 203-217
- [2] D. Auroux, *The canonical pencils on Horikawa surfaces*, *Geom. Topol.* **10** (2006) 2173-2217
- [3] D. Auroux and L. Katzarkov, *A degree doubling formula for braid monodromies and Lefschetz pencils*, *Pure Appl. Math. Q.* **4** (2008), no. 2, part 1, 237-318.
- [4] R. İ Baykur, *Inequivalent Lefschetz fibrations and surgery equivalence of symplectic 4-manifolds*, *J. Symplectic Geom.* **14** (2016), no. 3, 671-686.
- [5] R. İ Baykur, K. Hayano, and N. Monden, *Unchaining surgery and topology of symplectic 4-manifolds*, arXiv:1903.02906v2 [math.GT], March 2019.
- [6] K. Chakiris, *The monodromy of genus two pencils*, Ph.D. dissertation, Columbia University, 1978.
- [7] H. Endo, *Meyer's signature cocycle and hyperelliptic fibrations*, *Math. Ann.* **316** (2000), no. 2, 237-257.
- [8] H. Endo, *A generalization of Chakiris' fibrations*, in “Groups of Diffeomorphisms”, *Advanced Stud. Pure Math.* **52**, Math. Soc. Japan, Tokyo, 2008, 251-282
- [9] H. Endo, S. Nagami, *Signature of relations in mapping class groups and non-holomorphic Lefschetz fibrations*, *Trans. Amer. Math. Soc.* **357** (2005), no. 8, 3179-3199.
- [10] B. Farb and D. Margalit, *A primer on mapping class groups*, *Princeton Mathematical Series* **49**, Princeton University Press, 2012.
- [11] T. Fuller, *Diffeomorphism types of genus 2 Lefschetz fibrations*, *Math. Ann.* **311** (1998), 163-176.
- [12] T. Fuller, *Hyperelliptic Lefschetz fibrations and branched covering spaces*, *Pacific J. Math.* **196** (2000) 369-393.
- [13] T. Fuller, *Unchaining surgery, branched covers, and pencils on elliptic surfaces*, arXiv:2108.04868 [math.GT], August 2021. To appear, *Algebr. Geom. Topol.*
- [14] T. Fuller and I. Hadi, *The Alexander method and Lefschetz fibrations*, in preparation.
- [15] R. Gompf and A. Stipsicz, *4-manifolds and Kirby Calculus*, *Graduate Studies in Mathematics* **20**, American Mathematical Society, 1999.
- [16] I. Hadi, *New relations in mapping class groups*, M.S. thesis, California State University, Northridge, 2022.

- [17] M. Hughes, S. Kim, and M. Miller, *Isotopies of surfaces in 4-manifolds via banded unlink diagrams*, *Geom. Topol.* **24** (2020) 1519-1569.
- [18] T.-J. Li, *Smoothly embedded spheres in symplectic 4-manifolds*, *Proc. Amer. Math. Soc.* **127** (1999), 609-613.
- [19] B. Moishezon, *Complex surfaces and connected sums of complex projective planes*, *Lecture Notes in Math.* **603**, Springer Verlag, 1977.
- [20] B. Siebert and G. Tian, *On hyperelliptic C^∞ -Lefschetz fibrations of four-manifolds*, *Commun. Contemp. Math.* **1** (1999), no. 2, 255-280.
- [21] B. Siebert and G. Tian, *On the holomorphicity of genus two Lefschetz fibrations*, *Ann. of Math* (2) **161** (2005), no. 2, 959-1020.
- [22] I. Smith, *Lefschetz fibrations and the Hodge bundle*, *Geom. Topol.* **3** (1999), 211-233.
- [23] I. Smith, *Lefschetz pencils and divisors in moduli space*, *Geom. Topol.* **5** (2001) 579-608.

Terry FULLER

Department of Mathematics, California State University, Northridge,
Northridge, CA 91330

E-mail: terry.fuller@csun.edu